Tectonophysics xxx (2014) xxx–xxx

Contents lists available at ScienceDirect

Tectonophysics

journal homepage: www.elsevier.com/locate/tecto

Depth to Curie temperature across the central Red Sea from magnetic data using the de-fractal method

Ahmed Salem [a,b,c,*], Chris Green [a,b], Dhananjay Ravat [d], Kumar Hemant Singh [e], Paul East [a], J. Derek Fairhead [a,b], Saad Mogren [f], Ed Biegert [g]

[a] GETECH, Leeds, UK
[b] University of Leeds, Leeds, UK
[c] Nuclear Materials Authority, Cairo, Egypt
[d] University of KY, Lexington, USA
[e] Indian Institute of Technology, Bombay, Mumbai, India
[f] King Saud University, Saudi Arabia
[g] Shell International Exploration and Production, Houston, USA

ARTICLE INFO

Article history:
Received 28 May 2013
Received in revised form 25 February 2014
Accepted 18 April 2014
Available online xxxx

Keywords:
Magnetic
Curie
Depth
Heat flow
Red Sea

ABSTRACT

The central Red Sea rift is considered to be an embryonic ocean. It is characterised by high heat flow, with more than 90% of the heat flow measurements exceeding the world mean and high values extending to the coasts — providing good prospects for geothermal energy resources. In this study, we aim to map the depth to the Curie isotherm (580 °C) in the central Red Sea based on magnetic data. A modified spectral analysis technique, the "de-fractal spectral depth method" is developed and used to estimate the top and bottom boundaries of the magnetised layer. We use a mathematical relationship between the observed power spectrum due to fractal magnetisation and an equivalent random magnetisation power spectrum. The de-fractal approach removes the effect of fractal magnetisation from the observed power spectrum and estimates the parameters of depth to top and depth to bottom of the magnetised layer using iterative forward modelling of the power spectrum. We applied the de-fractal approach to 12 windows of magnetic data along a profile across the central Red Sea from onshore Sudan to onshore Saudi Arabia. The results indicate variable magnetic bottom depths ranging from 8.4 km in the rift axis to about 18.9 km in the marginal areas. Comparison of these depths with published Moho depths, based on seismic refraction constrained 3D inversion of gravity data, showed that the magnetic bottom in the rift area corresponds closely to the Moho, whereas in the margins it is considerably shallower than the Moho. Forward modelling of heat flow data suggests that depth to the Curie isotherm in the centre of the rift is also close to the Moho depth. Thus Curie isotherm depths estimated from magnetic data may well be imaging the depth to the Curie temperature along the whole profile. Geotherms constrained by the interpreted Curie isotherm depths have subsequently been calculated at three points across the rift — indicating the variation in the likely temperature profile with depth.

1. Introduction

The Red Sea represents an early stage in the break-up of a continental plate and the development of two divergent sub-plates. The crustal heat flow within the Red Sea is high with more than 90% of the measured values exceeding the world mean. The high heat flow values are not restricted to the axis of the Red Sea, but extend to the coasts where they are nearly twice the world mean (Girdler and Evans, 1977). Understanding the thermal structure of the embryonic continental margins and its local variations is an important factor in understanding the early stage of plate separation and identifying natural earth resources for the countries bordering the Red Sea. This requires building constrained thermal models of the lithosphere. The constraints include heat production and thermal conductivity at different levels, knowledge of seismic velocities at different depths, thickness of the crust and the lithosphere and estimates of basal heat flow into the lithosphere (Hemant and Mitchell, 2009; Ravat et al., 2011).

Spectral analysis of magnetic data can also help in the constraining of the temperature within the crust based on identifying and mapping the depth of the Curie isotherm. Above the Curie temperature, magnetic minerals lose their ferromagnetism. As magnetite is the most common magnetic mineral in the Earth's crust, the Curie temperature of magnetite, Tc = 580 °C, is commonly used to represent the Curie temperature of crustal rocks (e.g. Ross et al., 2006). This means that deeper layers at greater temperatures are essentially non-magnetic. This Curie isotherm interface can be detected through a number of spectral magnetic

* Corresponding author at. Getech, Kitson House, Elmete Hall, Elmete Lane, LEEDS, LS8 2LJ, UK; Switchboard: +44 113 3222200.
E-mail address: ahmed.salem@getech.com (A. Salem).

http://dx.doi.org/10.1016/j.tecto.2014.04.027
0040-1951/

methods (Bhattacharyya and Leu, 1977; Bouligand et al., 2009; Maus et al., 1997). The depth of the Curie isotherm is controlled by the variability of the geothermal heat flow from the mantle as well as from radioactive decay of minerals within the crust. Mapping the regional variation in the depth to the Curie isotherm provides an important constraint on temperatures within the Earth's crust and on maturation within sedimentary basins.

In this paper, we attempt to study the crustal thermal structure of the central Red Sea by determining the depth to the "magnetic bottom"; i.e. the base of the magnetised layer within the crust. We use the term "magnetic bottom" rather than the commonly used term "Curie isotherm depth", since the Moho or other crustal boundary can represent the bottom of the magnetic layer for petrological reasons (e.g. Rajaram et al., 2009; Ravat et al., 2011; Wasilewski et al., 1979). We estimate magnetic bottom using a new "de-fractal" spectral analysis approach applied to magnetic data. This approach assumes that the observed power spectrum is equivalent to the random magnetisation model multiplied by the effect of fractal magnetisation. This de-fractal approach removes the effect of fractal magnetisation from the power spectrum and estimates the parameters of depth to top and depth to bottom of the magnetic layer using iterative forward modelling of the power spectrum.

2. Spectral analysis

In the last four decades, variations on several methods have been proposed and applied for estimating the depth to the bottom (z_b) of magnetic sources using azimuthally averaged Fourier spectra of magnetic anomalies (e.g., Bhattacharyya and Leu, 1975; Bouligand et al., 2009; Fedi et al., 1997; Manea and Manea, 2011; Maus et al., 1997; Okubo et al., 1985; Rajaram et al., 2009; Ravat et al., 2007, 2011; Ross et al., 2006; Spector and Grant, 1970; Tanaka et al., 1999). The mathematical formulae of these methods are based on assumptions of flat layers with particular distributions of magnetisation, namely: 1) random (uncorrelated) magnetisation models or 2) self-similar (fractal) magnetisation models.

2.1. Random magnetisation models

Two types of method have been commonly used in the spectral estimation of z_b (depth to bottom of the magnetic layer) assuming random magnetisation models: (a) the spectral peak method originally described in a landmark paper by Spector and Grant (1970) and used by Shuey et al. (1977), Connard et al. (1983), Blakely (1988) and Salem et al. (2000) among others and (b) the centroid method originally presented by Bhattacharyya and Leu (1977), Okubo et al. (1985), and Tanaka et al. (1999). Both methods need a priori – generally independent – estimation of the depth to the top (z_t) of the magnetised layer, although a development by Ross et al. (2006) and Ravat et al. (2007) proposed methods to estimate depths to the top and the bottom of the magnetic layer simultaneously in cases where spectral peaks are observed. Theoretically, the power–density spectrum of the observed magnetic field is given by Blakely (1995) as

$$\Phi\left(k_x, k_y\right) = A\left(k_x, k_y\right)\Phi_M\left(k_x, k_y\right)\left(e^{-kz_t} - e^{-kz_b}\right)^2 \quad (1)$$

where $\Phi_M(k_x, k_y)$ is the power–density spectrum of magnetisation, $A(k_x, k_y)$ is a function that depends on the vector directions of magnetisation and ambient field (Blakely, 1995), z_t and z_b are, respectively, the depth to the top and the depth to the bottom of the magnetised layer, k_x and k_y are wavenumbers in the x and y directions respectively and

$$k = \sqrt{{k_x}^2 + {k_y}^2}. \quad (2)$$

is the radial wavenumber. For estimating the depth to the top of a magnetic layer, Spector and Grant (1970) showed that the slope of the logarithm of the azimuthally averaged Fourier power spectrum of magnetic anomalies from an ensemble of simple sources, at mid to high wavenumbers, is related to the depth to the top of the ensemble:

$$\log\left[\overline{\Phi}(k)\right] = B_1 - 2kz_t, \quad (3)$$

where B_1 is a constant. According to Blakely (1995), if the magnetic data set is large enough such that the low-frequency anomalies caused by the bottom of the source are included in the anomaly map (Connard et al., 1983), a peak should be evident in the spectrum, whose central wavenumber relates to the depth of the bottom of the sources (Spector and Grant, 1970). The observed spectral peak position (k_{peak}) is a function of z_t and z_b and is given by the following equation (Blakely, 1995; Connard et al., 1983)

$$k_{peak} = \frac{\log(z_b) - \log(z_t)}{z_b - z_t}. \quad (4)$$

Bhattacharyya and Leu (1977) presented a method for the determination of the depth to the centroid of a rectangular parallelepiped with uniform magnetisation, which they had used earlier in their study of Curie isotherm depths of the Yellowstone Caldera (Bhattacharyya and Leu, 1975). Okubo et al. (1985) expanded their method to ensembles of sources with random magnetisation. In this method, the estimate of the depth to the centroid (z_c) is obtained from the logarithm of an azimuthally averaged wavenumber-scaled Fourier amplitude spectrum in the low wavenumber region such that

$$\log\left[\overline{\Phi}(k)^{1/2}/k\right] = B_2 - kz_c, \quad (5)$$

where B_2 is a constant. Once the centroid depth is obtained from Eq. (5) and the estimate of the depth to the top of the source is obtained from Eq. (3), the depth to the bottom of the magnetic layer can simply be calculated as

$$z_b = 2z_c - z_t. \quad (6)$$

The above two methods assume a layer of random magnetisation. In some cases, these methods may lead to incorrect determinations of the Curie isotherm depth/magnetic bottom if the layer has fractal magnetisation (Bouligand et al., 2009; Maus et al., 1997) or it is made up of an ensemble of sources with different dimensions than those implicit in the method of Spector and Grant (Fedi et al., 1997).

2.2. Fractal magnetisation models

The idea of using models with fractal magnetisation distribution comes from the concept of self-similarity (Kolmogorov, 1941; Mandelbrot, 1983), which is consistent with susceptibility logs (Maus and Dimri, 1995; Pilkington and Todoeschuck, 1993), susceptibility surveys (Pilkington and Todoeschuck, 1995) and magnetic maps (Maus and Dimri, 1994, 1995; Pilkington and Todoeschuck, 1993). Based on this concept, Maus et al. (1997) derived a spectral density model for the anomaly of the total intensity of the magnetic field. The model accounts for the self-similarity as well as the limited depth extent of the crustal magnetisation. The theoretical power spectrum due to a slab of self-similar magnetisation distribution is given by Maus et al. (1997) as

$$\frac{1}{2\pi}\int_0^{2\pi} \ln\left[\Phi\left(k_x, k_y\right)\right] d\theta = B_3 - 2kz_t - tk - \beta \ln(k) + \ln\left[\int_0^{\infty} [\cosh(tk) - \cos(tw)]\left(1 + \frac{w^2}{k^2}\right)^{-1-\beta/2} dw\right] \quad (7)$$

Please cite this article as: Salem, A., et al., Depth to Curie temperature across the central Red Sea from magnetic data using the de-fractal method, Tectonophysics (2014), http://dx.doi.org/10.1016/j.tecto.2014.04.027

where θ is the angle from k_x, B_3 is a constant related to magnetisation, t is the thickness of the slab, w is the wavenumber in the z direction, and β is fractal index describing the degree of self-similarity of the magnetisation. For example, $\beta = 1$ is very close to the random magnetisation model assumed by Spector and Grant (1970) as shown in Bouligand et al. (2009). Higher β values represent increasingly correlated magnetisation variation. An increase in the fractal index β of magnetisation increases the slopes of the power spectrum and generally z_t and z_b will be overestimated if we assume a lower fractal index.

Bouligand et al. (2009) derived an analytical solution for the integral derived in Eq. (7) which involves three parameters: the depth to the top of the magnetic layer, z_t, the layer thickness, t, and the fractal magnetisation parameter, β. The analytical solution allowed faster computations that made possible the application of the method to a large grid of magnetic data in a moving window manner (Ravat et al., 2011). However, the fractal parameter and the depth to the top of the magnetic layer are interdependent and strongly correlated (Bouligand et al., 2009). Ravat et al. (2011) found the automatic non-linear parameter estimation approach less reliable because the shape of the misfit residual is open-ended toward greater thicknesses and there is a range of reasonable solutions that lead to similar residual misfits to the observed spectrum. Even though the minimum norm criterion may lead to a single solution within realistic bounds, it does not mean that this solution is unique and is the correct one. We advocate visual inspection and user selection (Ravat et al., 2011) rather than the use of automatic methods to determine the solution, for several reasons:

- the scientific problem is non-unique and additional external information must be taken into account in constraining the solution;
- the misfit norm, and therefore the minimum misfit, is dependent on the choice of the wavenumber range over which the misfit is computed;
- there are a number of misfit norms (L1, L2, C-norm, etc.), and the minimum misfit for each of them results in different solved parameters (in this case, different z_t, t and β);
- it is not clear at this point that any one of the norms is superior to the others for this problem;
- the user can take account of reasonableness of solutions as well as irregularities with the data and the spectrum in making their selection.

Here we develop an alternative approach, which we call the "de-fractal" method or "de-fractal spectral depth determination" method, that can reduce the ambiguity in the selection of the fractal parameter, and in doing so can provide z_b estimates that are more reasonable than those estimated using conventional methods.

3. The de-fractal spectral depth determination method

The de-fractal method is based on the assumption that the observed power spectrum is adequately represented by a simplification of the fractal magnetisation power spectrum where the magnetisation in the x and y directions is fractal and is constant in the z direction. In this case, the observed power spectrum is equivalent to the result of power spectral density of the random magnetisation model multiplied by $k^{-\alpha}$ such that

$$\Phi_F\left(k_x, k_y\right) = \Phi_R\left(k_x, k_y\right)k^{-\alpha}, \tag{8}$$

where $\Phi_F(k_x, k_y)$ is the observed power spectrum, $\Phi_R(k_x, k_y)$ is the power spectrum due to the random magnetisation model, k is the radial wavenumber, and α is the fractal index $\alpha = \beta - 1$ (Maus and Dimri, 1994), where β is the fractal parameter of magnetisation. If we can determine the value of α, we can "de-fractal" the observed power spectrum by multiplying it by the factor k^{α} and extract a power spectrum equivalent to the random magnetisation version as follows

$$\Phi_R\left(k_x, k_y\right) = \Phi_F\left(k_x, k_y\right)k^{\alpha}. \tag{9}$$

Having removed the fractal effect, we can treat the resulting de-fractal power spectrum as though it was the power spectrum of a random magnetisation model. The present approach can be considered as a correction to the power spectrum of the field for the fractal distribution of magnetisation. The concept of correcting the power spectrum is not new. Fedi et al. (1997) and Ravat et al. (2007) have used a similar approach and estimated depth to the top to the magnetic layer from a corrected power spectrum. Bansal et al. (2011) corrected the power spectrum to modify the scaled power spectrum and modified the centroid method for fractal distribution.

The present approach utilises all previous techniques and integrates the spectral peak and centroid methods in an interactive forward modelling approach. We de-fractal the power spectrum by a range of α parameters and examine them for under- or over-correction. The viable values of α are those where the expected peak is present in the de-fractal power spectrum. We choose the correct α based on visual inspection of the fit between the de-fractal power spectrum and the modelled power spectrum. For sufficiently large windows, random magnetisation would result in a peak in the observed field spectrum (the width of the window would generally need to be around six times the depth to the bottom of the magnetic layer); therefore if the peak is not seen in the observed spectrum, it could be due to the fractal nature of magnetisation.

Fig. 1 shows a flowchart of the de-fractal approach for estimating z_b. We first start with a tentative low value of α and then we perform the de-fractal transformation on the observed power spectrum. We then apply the fractal centroid method and estimate z_t based on fitting the linear segment in the mid to high wavenumber range of the power spectrum and estimate the centroid depth by fitting the linear segment in the low wavenumber range of the scaled power spectrum.

Fig. 2A shows an example of the magnetic field due to a fractally magnetised layer with $z_t = 10$ km, $z_b = 20$ km, and $\alpha = 3$ ($\beta = 4$). To calculate the synthetic magnetic data for a fractal magnetisation model, we follow the approach of Pilkington et al. (1994) by generating magnetisation with Gaussian random noise and then multiplying its Fourier transform by $k^{-\alpha}$. Fig. 2B shows the radially averaged power spectrum of the calculated magnetic data.

To demonstrate the method, we applied the de-fractal approach using different α values starting from 1. We estimated z_t and z_b using Eqs. (3), (5), and (6) for each de-fractal power spectrum (Table 1).

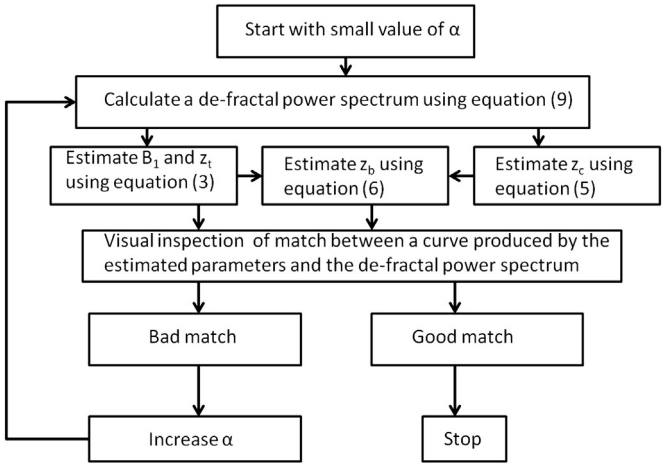

Fig. 1. Flowchart of the de-fractal approach for estimating depth to magnetic bottom.

Please cite this article as: Salem, A., et al., Depth to Curie temperature across the central Red Sea from magnetic data using the de-fractal method, Tectonophysics (2014), http://dx.doi.org/10.1016/j.tecto.2014.04.027

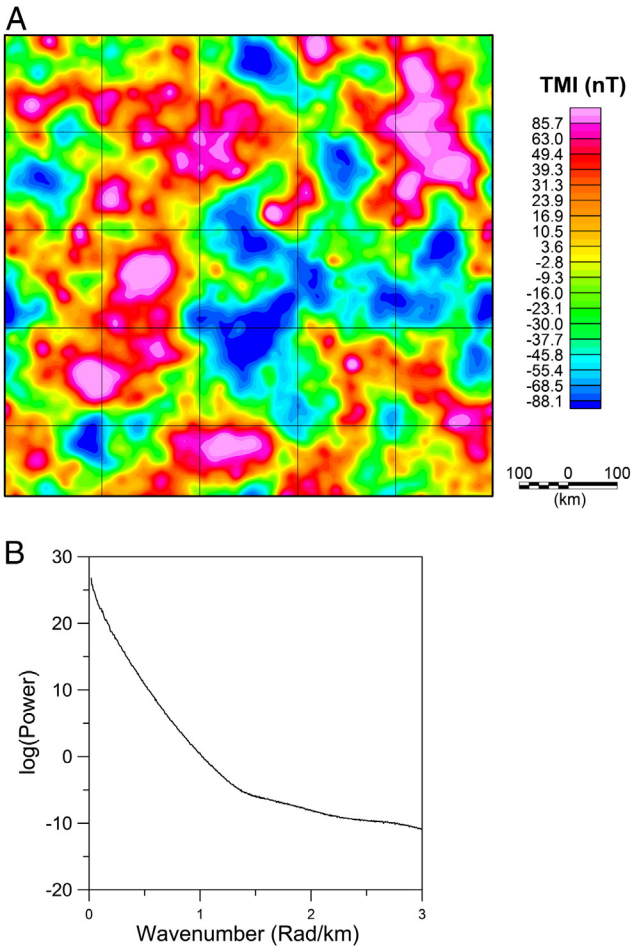

Fig. 2. A) Total magnetic intensity map for a fractal magnetisation ($\alpha = 3$) model with depth to the top and bottom of the magnetic layer of 10 km and 20 km respectively. B) Radially averaged power spectrum of the model magnetic data in panel A.

The application of the method does not involve a priori knowledge of the fractal magnetisation parameter, α. We also use 1/k scaled de-fractal spectra to determine the centroid depth from the de-fractal centroid method, since both peak modelling and the centroid methods are consistent with each other. The match between the modelled power spectrum and the de-fractal spectrum (Fig. 3) improves gradually until a good fit is obtained using the fractal value of $\alpha = 3$. The goodness of fit is assessed visually taking into account the main features along the whole power spectrum with particular focus on the longest wavelengths and ignoring local excursions in the power spectrum. To ensure that other possible solutions corresponding to higher values of fractal exponent are not missed, we used a higher fractal value of $\alpha = 4$ and determined z_t and z_b from the de-fractal centroid method as before. A mismatch was found between the modelled power spectrum and the de-fractal spectrum (Fig. 3D). This indicates that the cross-checking between both the peak modelling and the centroid methods guards against erroneous results.

Table 1
Results of estimating depth to top and depth to bottom using different de-fractal values from the power spectrum of the theoretical magnetic data over fractal magnetisation model ($\alpha = 3$) with a depth to the top of 10 km and depth to bottom of 20 km.

Fractal index (α)	z_t (km)	z_b (km)
1	11.7	48.2
2	10.6	34.7
3	9.7	21.0
4	8.4	10.9

The result of this model example (Table 1) is accurate to within 10% of the actual depth values; this can also be assessed by manual fitting of power spectra from a number of different models. Experience has shown that in practice, the error can be large, but is not biased to give either consistently deeper or shallower results (i.e. the error is effectively random). Thus we consider this model example to be adequately representative of the true underlying function of the method in the vast majority of practical situations. However, scenarios exist that will cause the method to fail. Where the cumulative effects of errors in the data or real-world deviations from the model assumptions exceed the signal from the geological depth to Curie isotherm, we can say that the model has failed, otherwise we say that the data are within the operating requirements of the de-fractal method. Where the following (most commonly encountered) issues have a great influence in the input data set, we can generally infer that the model will fail:

- Poor quality surveys integrated into a compilation grid
- Inconsistencies when multi-survey compilations are stitched together, altering the long-wavelength part of the spectrum
- Different processing applied to the compiled grid
- Severity of data gaps (and their inadequate interpolation) in the selected data window
- Window size inadequate for vertical resolution of z_b; generally a window of at least six times the depth is desirable.
- Regions which differ from our model assumptions (e.g.: more than one geological regime in the selected window with different fractal properties of source magnetisations or significantly higher magnetisation top layer overlying normal magnetisation).

4. Depth to magnetic bottom in the central Red Sea

The central Red Sea was chosen to demonstrate the de-fractal approach, because the depth to the Curie isotherm is expected to vary significantly in a traverse from the African continent to the new oceanic crust of the Red Sea to the Arabian continent; there is also a continuous band of magnetic data available across the central Red Sea. Various aspects of the evolutionary history of the Red Sea are still debated — including the impact of thermal forcing from a mantle plume. Rifting probably initiated ~25 Ma (Bosworth et al., 2005); sea-floor spreading (i.e. generation of oceanic crust) happened much later — probably 5–10 Ma. Currently, the Arabian plate is moving away from the African plate with an Euler pole in NE Libya ~(24.5°E, 31.5°N) and rotation ~0.37°/Ma (ArRajehi et al., 2010). This implies a full drift rate of ~10 mm/year in the central Red Sea which approximately fits with the ~80 km of ocean crust modelled by Salem et al. (2013) based on gravity data. The north end of the Red Sea is covered with thick sediments which are commonly believed to be underlain by stretched continental rather than oceanic crust. Magmatic and seismic evidence indicates that the axis of the southern Red Sea is no longer active, but extension is now taken up in the Danakil Rift to the west (Bastow and Keir, 2011). Thus the central Red Sea is the only currently active section of ocean and hence the most suitable for this study.

We have estimated the depth of "magnetic bottom" along a SW–NE profile crossing the central Red Sea at 22°N, 38°E. The total magnetic intensity data set shown in Fig. 4 has been compiled from three data sources:

- On the Sudan side of the Red Sea, the data were derived from a V/O Technoexport survey acquired in 1971 for the Sudan Ministry of Industry and Mining with flight line spacing 2 km, line direction N90° and a flying height of 300 m.
- Over the Red Sea, the data are from a survey acquired in 1976 for the Red Sea Saudi–Sudanese Commission (RSC) with flight line spacing 10 km, line direction N60° and a flying height of 305 m.
- On the Saudi Arabia side of the Red Sea, the data form part of a major Arabian Shield survey flown in part by Hunting in 1965–1966 with flight line spacing 500–800 m and line direction N30° at 150 m elevation.

Please cite this article as: Salem, A., et al., Depth to Curie temperature across the central Red Sea from magnetic data using the de-fractal method, Tectonophysics (2014), http://dx.doi.org/10.1016/j.tecto.2014.04.027

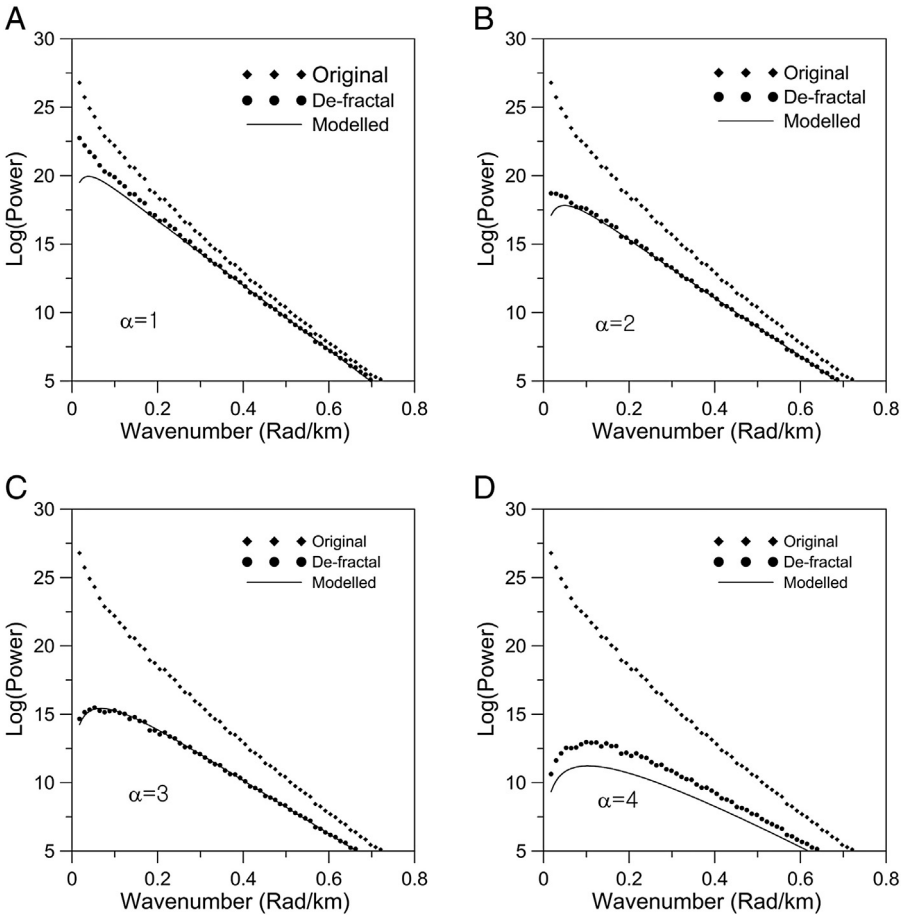

Fig. 3. Comparison of de-fractal power spectra of the power spectrum in Fig. 2B using different α values (1, 2, 3 and 4) and modelled curves produced using the best fit estimated parameters (Table 1).

The Sudan and Red Sea surveys formed part of Getech's African Magnetic Mapping project (AMMP) (Getech, 1992; Green et al., 1992) and the Saudi surveys are from Mogren (2004). The data were integrated as a grid with 1 km cell size and are presented at a height of 1 km above land or sea surface — based on upward continuation as appropriate. In our application, 12 overlapping sub-windows were extracted

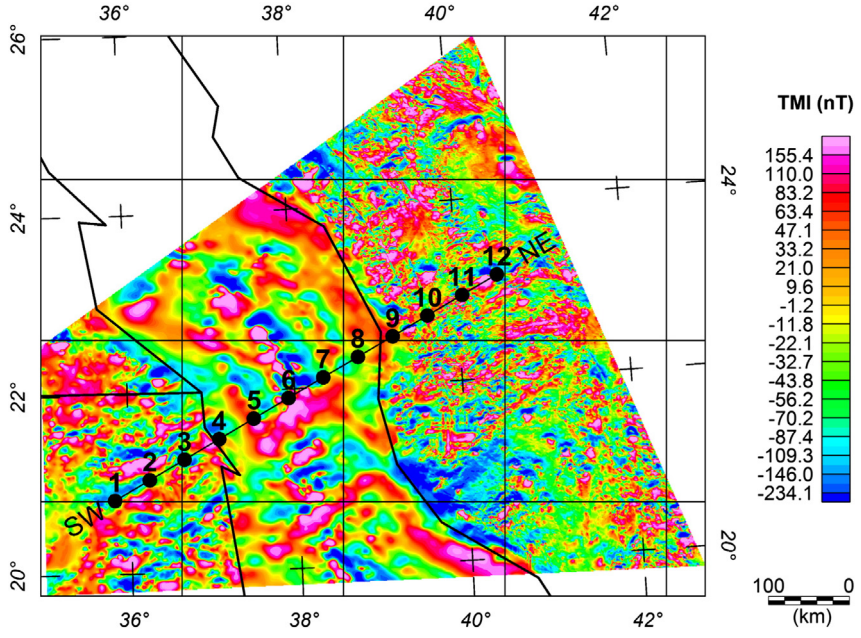

Fig. 4. Compilation of aeromagnetic data over central Red Sea. Numbers indicate the centres of windows analysed for estimating depth to Curie isotherm.

Please cite this article as: Salem, A., et al., Depth to Curie temperature across the central Red Sea from magnetic data using the de-fractal method, Tectonophysics (2014), http://dx.doi.org/10.1016/j.tecto.2014.04.027

Table 2
Results of estimating depth to top and bottom of the magnetic layer in the central Red Sea. Depths are below sea level.

Window number	De-fractal method			Centroid method	
	Fractal index (α)	z_t (km)	z_b (km)	z_t (km)	z_b (km)
1	0.8	1.5	16.4	1.5	20.9
2	0.6	1.6	18.9	1.7	20.0
3	0.7	1.0	16.2	1.5	17.1
4	0.7	2.5	16.8	4.0	18.5
5	1.0	2.8	10.3	3.9	20.9
6	1.7	2.9	8.4	4.4	25.5
7	1.4	2.8	9.3	4.0	23.8
8	1.4	3.1	14.5	5.0	27.3
9	0.9	0.9	17.8	2.2	21.5
10	0.7	1.3	17.1	2.2	20.6
11	0.0	1.2	11.8	1.2	11.8
12	0.3	1.3	13.9	1.4	14.9

from the magnetic grid of the central Red Sea area for estimating depth to the top and bottom of the magnetic layer using the de-fractal approach. To select the optimum window size for spectral analysis from each window, we reviewed previous studies by several authors (Blakely, 1995; Maus et al., 1997; Ravat et al., 2007). Blakely (1995) showed that the grid dimension should be five times z_b. Ravat et al. (2007) suggested based on practical experience that the grid dimension should be no less than 200–300 km for an average Moho or Curie isotherm depth of roughly 30 km and preferably 10 times the depth to the bottom. Maus et al. (1997) recommended that the grid dimension should not be less than 1000 km. In the Red Sea region, it is expected that the depth of magnetic bottom is shallow due to either shallow depth of Moho and/or shallow depth of Curie temperature. Therefore, we used a small window size of 100 km by 100 km with an overlap of 50 km. Although the maximum estimate of the depth to bottom will be limited using this window size, the spatial resolution achieved in mapping the depth to bottom will be enhanced.

For each window, a first order trend was removed from the data and a power spectrum was then calculated using the fast Fourier transform (FFT). We applied the de-fractal method as shown in Fig. 1 to each power spectrum using different α values and estimated associated values of depth to top and depth to bottom of the magnetic layer. Selection of the wavenumber range is important for calculating the depth to top and depth to bottom of the magnetic layer from the power spectrum. The selection always requires careful judgement and it is valuable to have some independent information to constrain the results. Concerning the depths to the top of magnetic layer, Tanaka et al. (1999) suggest computing z_t from the high-wavenumber part of the spectrum. Calculating the depth to the top of magnetic layer from the higher wavenumber portion may be appropriate for identifying the depth to the shallowest magnetic material, if one is mapping a single layer representing the bulk of the magnetisation. We use the straight-slope part of the spectrum next to the peak (from wavenumbers higher than the peak) to estimate the depth to the top of the single layer or the deepest magnetic layer in multi-layer situations. This is important because multi-layer magnetisation situations are common, especially in continental areas and in those cases, to determine the magnetic bottom, one needs to select the slope related to the deepest magnetic layer (we encounter the multi-layer situation in the analysis of windows 11 and 12). One of the advantages of the de-fractal method is that this slope segment is simple to identify in the above manner because the de-fractaled spectrum always has a peak. On the other hand, the identification of the slope related to the top of the deepest layer is not always possible through any other fractal consideration, especially because the lowest wavenumber portion of the spectrum is the most noise-prone as it has the fewest intrinsic spectral estimates and can be mistaken for a "ghost" layer deeper than the strongest, deepest magnetic layer. We used the wavenumber range corresponding to >20 km wavelength to estimate the centroid depth and different α values starting from zero.

Table 2 lists the estimated results for fractal index α, depth to the top and depth to bottom of the magnetic layer. We did not find a clear spectral peak in most of the original power spectra except window 11. Spectral peaks in the power spectrum are only found for random magnetisation distribution and in some cases when the magnetisation distribution is associated with low values of fractal index. Figs. 5 to 7 show examples of the power spectra onshore Sudan, central Red Sea, and onshore Saudi Arabia. We observed that the peak in the power spectrum is not well constrained in some spectra, especially on the onshore Sudan side. This may be attributed to deviation of the magnetisation distribution from our assumed model or due to magnetic data of lesser quality on the Sudan side.

For window 11 onshore Saudi Arabia, we estimated the depth to the top and depth to bottom from the original power spectrum without any de-fractal process. A good match was obtained between a curve of the estimated parameters and the original power spectrum. This indicates that the magnetisation distribution in this location can be treated as a random distribution. Observing this peak also implies that the true bottom is sensed by the 100 km window. For the other spectra, we found that the optimum α values are generally small and between ($\alpha = 0.3$) and ($\alpha = 1.7$). Bouligand et al. (2009) reviewed the fractal parameters derived from aeromagnetic studies in continental domains and found a large range of values obtained from computational windows with dimensions from 50 km to 4000 km. Their tabulation of various studies suggests a value of $\beta = 4$ as representative of the fractal parameter for deep crustal magnetisation in continental domains.

Spectra in onshore areas on both the African and Arabian sides require small α values, whilst spectra in the Red Sea rift require higher α values. This result is not surprising as one should expect the magnetic

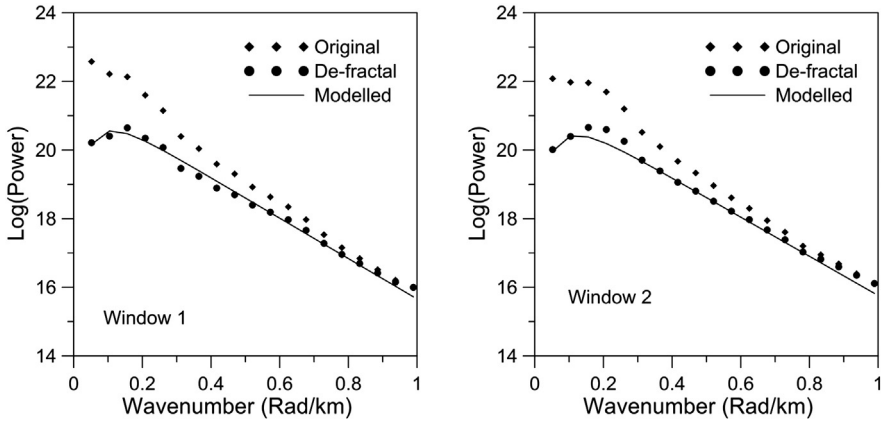

Fig. 5. Spectra of 100 km square windows from the onshore Red Sea on the African side. Window numbers indicate locations of the centres of the windows in Fig. 4.

Please cite this article as: Salem, A., et al., Depth to Curie temperature across the central Red Sea from magnetic data using the de-fractal method, Tectonophysics (2014), http://dx.doi.org/10.1016/j.tecto.2014.04.027

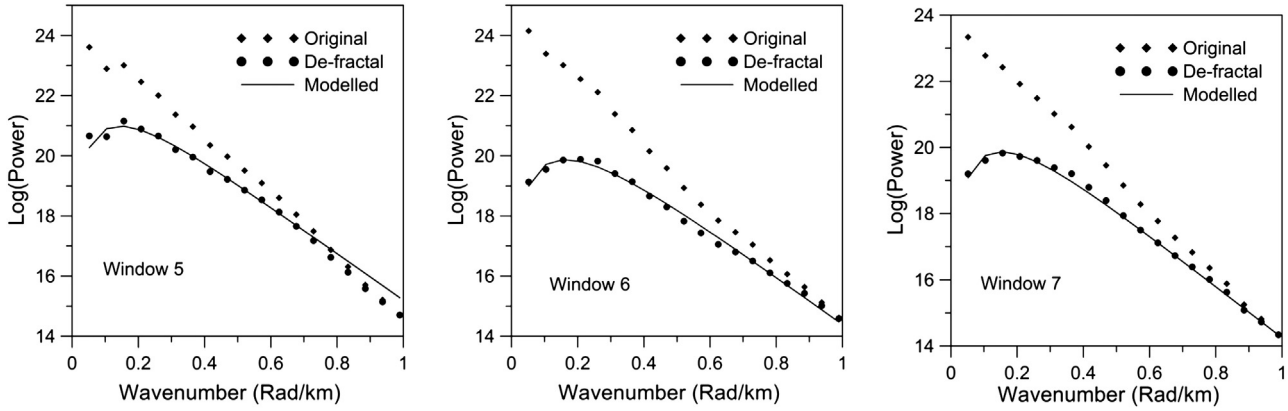

Fig. 6. Spectra of 100 km square windows from offshore Red Sea window numbers indicate locations of the centres of the windows in Fig. 4.

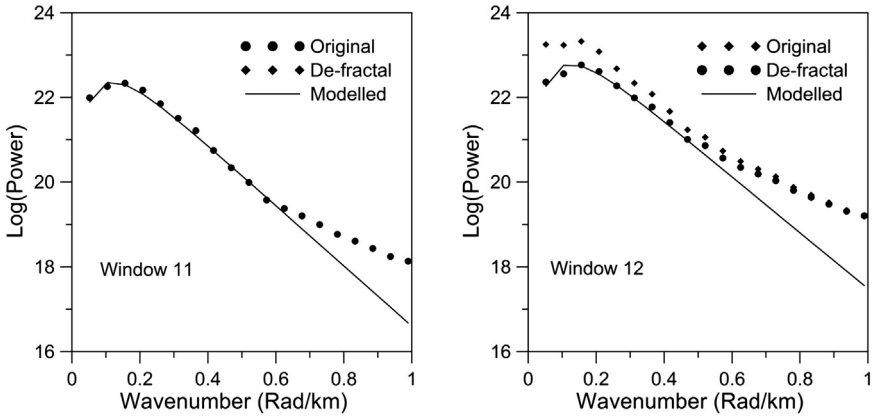

Fig. 7. Spectra of 100 km square windows from the onshore Red Sea on the Arabian side. Window numbers indicate locations of the centres of the windows in Fig. 4.

pattern of the rocks in the continental area to be completely different from that in the oceanic area. The estimate of the depth to top is relatively flat across the whole profile, although the aeromagnetic data suggest an abrupt change with longer wavelength magnetic anomalies offshore (windows 4–8); this is reasonable due to the differences in the magnetic line spacing, although the consistency of the depths suggests stability in the depth estimation process. However, a 100 km window will lead to smoothing of the depth to the top of magnetic layer especially if it is shallow as in this study.

For comparison, we estimated depth to bottom from the same spectra using the classical centroid method (Okubo et al., 1985) — without any de-fractal process (Table 2). The magnetic bottom depths using the classical centroid method would have been overestimated by up to 17 km in the rift area. Generally, the results of the de-fractal method seem to be reasonable as shallower depth to bottom was estimated in the rift area and deeper depths were estimated in the onshore area. We have also computed lithospheric temperatures with increasing distance/age from the centre of the Red Sea based on the thermal boundary layer cooling half-space model (Davis and Lister, 1974; Stein and Stein, 1992) assuming 10 Ma of spreading. The implied depths of the 580 °C isotherm at the window locations near the rift area (5, 6, and 7) are 11.9 km, 1.4 km, 10 km, respectively. These estimated depths are consistent with our depth to the bottom estimates from the de-fractal method (except toward the centre of the rift where the half-space thermal model is likely to be inappropriate).

To better determine the local depth we have computed the depth to the top of the magnetic layer using the tilt–depth method (Salem et al., 2007) for each data window. Tilt–depth is a simple method to estimate depth to the top of magnetic sources from derivatives of the magnetic field. Fig. 8 shows differences in the depths derived from the spectral and tilt–depth methods. In the offshore area, the results are close to each other, but in the onshore areas results of the spectral analysis are deeper indicating that there are shallow magnetic sources which do not necessarily impact the depth range of the major crustal magnetic layer. Despite this, lower spatial resolution (i.e., longer wavelengths) of the Red Sea portion of the magnetic anomaly data could cause deepening of the depths to the top of the magnetic layer derived in this study (i.e., windows 4 to 8).

Fig. 9 shows the estimate of the depth to Curie isotherm (depth to bottom) for this study and the depth to the Moho from 3D inversion of gravity data calculated by Salem et al. (2013). This study shows that the estimate of the depth to magnetic bottom is always shallower than the depth to the Moho except possibly close to the rift axis where these two surfaces coincide. An interesting result is that the

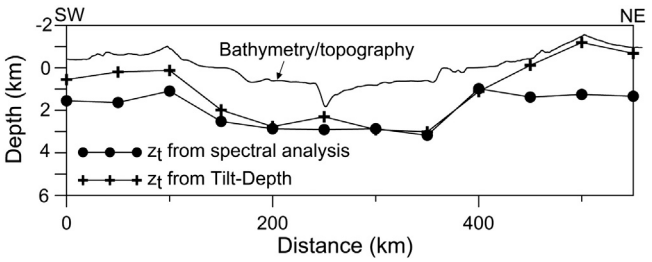

Fig. 8. Depth to the top of the magnetic layer based on spectral analysis and depth to top of magnetic sources based on tilt–depth method (Salem et al., 2007). Depths are below sea level.

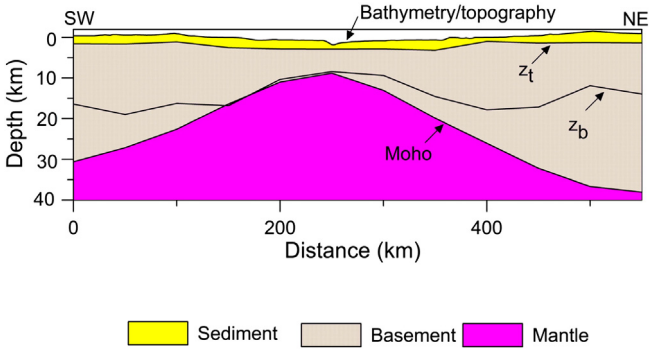

Fig. 9. Crustal thickness across the Red Sea: Depth to Moho based on 3D inversion of gravity data constrained using seismic refraction and receiver function results (Salem et al., 2013). Depths are below sea level.

depth of the Curie temperature becomes significantly shallower than the Moho with distance from the spreading axis of the Red Sea. The depth of the Curie temperature stays at about 15 to 20 km whilst the Moho steadily increases to 30 km and slightly greater at the coast lines. This relationship suggests that the magnetic bottom represents the depth to Curie isotherm in the continents and margins, but in the rift it is less conclusive and the depth to bottom may just mark a petrologic boundary — the Moho.

Generally, oceanic plates have most of the magnetisation concentrated in the first 2 km or so in the basaltic crust (layer 2). However, because of the extremely slow spreading, we expect that the central portion of the Red Sea consists primarily of intrusives and not the normal oceanic layering. Depth to Curie temperature was estimated in a more northerly segment of the Red Sea (the western margin of the Red Sea near Egypt) by Ravat et al. (2011) using the fractal (not de-fractal) and the centroid methods. They found both shallow and deep magnetic bottom depths in a more northerly segment of the Red Sea, where the deep estimates are significantly deeper than the Moho suggesting that oceanic uppermost mantle may be serpentinised to a depth of 15–30 km in those locations. However, our results indicate that in the rift area in the central Red Sea segment we have analysed, the Curie temperature and the Moho are at the same level.

5. Curie isotherm depth estimation from heat flow data

The depths to Curie isotherm from the analysis of magnetic data can be compared with values estimated from an alternative approach using surface heat flow observations combined with a careful analysis of local rock properties — especially thermal conductivity and radiogenic heat production. This approach has been demonstrated by Hemant and Mitchell (2009) who calculated the depth of the Curie isotherm within the Tibetan plateau and Himalayan mountains using surface heat flow data and gross thermal properties of the region. Here we use similar methodology to calculate Curie isotherm (assumed to be 580 °C) depths within the Red Sea region and adjoining continental regions of Arabia and Africa based on heat flow measurements.

The Curie temperature in the subsurface is influenced by the thermal conductivity and radiogenic heat production of the rocks through the lithosphere. The heat conduction equation (Fowler, 2005) describes the rate of change of temperature, T, with time, t, at any point as

$$\frac{\partial T}{\partial t} = \frac{k}{\rho C_p}\nabla^2 T + \frac{A}{\rho C_p}, \tag{10}$$

where A is the radiogenic heat production, k is the thermal conductivity, ρ is the density and C_p is the specific heat capacity of the material. In steady state conditions, $\partial T/\partial t = 0$ (equilibrium geotherm) the equation simplifies to:

$$\nabla^2 T = -\frac{A}{k} \tag{11}$$

or, in the 1D vertical approximation, to

$$\frac{\partial^2 T}{\partial z^2} = -\frac{A}{k}. \tag{12}$$

A local 1D Earth model can be built based on a series of horizontal layers each with typical values of A and k. The temperature–depth profile through such a model is obtained by applying boundary conditions for temperature and heat flow at the surface and ensuring continuity of temperature and heat flow at all the subsequent intermediate surfaces. The resulting equations can then be employed to compute the temperature variation with depth below each measurement point and hence estimate the depth to the Curie isotherm.

In this study, a three layer model was used. Bulk thermal properties were estimated for each geological unit based on random distribution of typical rock types in the area (Roy et al., 1981) and the observed thermal properties of different rocks and minerals (e.g. Clauser and Huenges, 1995). The thermal conductivities and the radiogenic heat production values for layer 1 are based on the surface geology of the region (CCGM, 2000). In areas of sedimentary outcrop, this surface geology is the sediment layer whose thickness is defined by the sediment thickness map of Bassin et al. (2000). Within the continental region, layer 2 is the basement geology which is represented by the major geological units obscured beneath the sediments, although in this area the sub-sedimentary basement is not well mapped and a constant value is used. In the ocean layer 2 is basalt (White et al., 1992). The third layer within the continents is mainly granulites and granodiorites whilst within the ocean it is gabbro. The thermal properties of all these layers are shown in Table 3. The thicknesses of layer 2 and layer 3 are taken from the thickness model of upper and lower crust (Nataf and Richard, 1996) respectively.

In an area with a good distribution of reliable heat flow measurements, it is possible to use this approach to build a map of depth to Curie isotherm which can be compared against the Curie isotherm depth mapped from magnetic data. In this area, the available heat flow data set is limited, which limits our ability to map the Curie isotherm depth using this technique; however a small number of individual data points can be used as an indicative comparison of the techniques. We used heat flow observations from the International Heat Flow Commission (available to download from http://www.heatflow.und.edu) which includes various data compilations, including the compilation of Pollack (1992).

The locations of the surface heat flow observations are shown in Fig. 10. Most of these observations are located along the central regions of the Red Sea whilst only a few are in the continental regions. Based on the 1D model and the thermal properties identified above, Curie isotherm depths could be calculated at each point. However, inspection of the actual heat flow values indicates that the data along the axis of the ridge (where most of the points are located) are highly variable; for example the small cluster of points around 38.1°E, 21.4°N has recorded heat flow values from 29 $mW \cdot m^{-2}$ to 3300 $mW \cdot m^{-2}$. Information about the measurements, the errors and the sampling strategy are not available, so it is difficult to assess these data. It is well known that active magmatic processes occurring at mid-ocean ridges will generate variable and locally extreme heat flow values. Thus, the apparent variability in heat flow may be real, but the heat flow in such situations will probably not be indicative of heat transport by conduction at a regional crustal scale, indeed it may indicate that the heat flow is not steady-state nor 1D. It is clear, therefore, that heat flow values along the central axis of the Red Sea can only provide a general indication of

Please cite this article as: Salem, A., et al., Depth to Curie temperature across the central Red Sea from magnetic data using the de-fractal method, Tectonophysics (2014), http://dx.doi.org/10.1016/j.tecto.2014.04.027

Table 3
Thermal properties assigned for rocks in the Red Sea region — based on surface geology and deep crustal models.

	Ocean			Continent		
	Rock	k	A	Rock	k	A
Layer 1	Mapped sedimentary geology	1.1–2.5 $W \cdot m^{-1} \cdot K^{-1}$	1.2–2.4 $\mu W \cdot m^{-3}$	Mapped sedimentary geology	1.1–2.5 $W \cdot m^{-1} \cdot K^{-1}$	1.2–2.4 $\mu W \cdot m^{-3}$
Layer 2	Basalt	2.40 $W \cdot m^{-1} \cdot K^{-1}$	0.55 $\mu W \cdot m^{-3}$	Mapped basement geology	2.73 $W \cdot m^{-1} \cdot K^{-1}$	0.55 $\mu W \cdot m^{-3}$
Layer 3	Gabbro	2.60 $W \cdot m^{-1} \cdot K^{-1}$	0.55 $\mu W \cdot m^{-3}$	Granulite & granodiorite	2.45 $W \cdot m^{-1} \cdot K^{-1}$	0.55 $\mu W \cdot m^{-3}$

the temperature with depth. The median value of 160 $mW \cdot m^{-2}$ was chosen to represent the heat flow in the centre of the Red Sea.

Onshore Sudan, close to the coast, there is a cluster of three points (Fig. 10) with heat flow values of 100 $mW \cdot m^{-2}$, 100 $mW \cdot m^{-2}$ and 89 $mW \cdot m^{-2}$, which are reasonably close to the magnetic profile. As the scatter is small, these data are considered reliable and an average value of 96 $mW \cdot m^{-2}$ is used to represent this area.

In Saudi Arabia there is only one onshore point anywhere near to the profile. This point (Fig. 10) has a heat flow value of 50 $mW \cdot m^{-2}$, but it is considered to be of limited value, because it is a single isolated point with no corroboration and is far away from the magnetic profile. The results from analysing these few heat flow observations are shown in Table 4. If we make the assumption that the structure is mainly 2D in the area, we can indicate which magnetic window we expect to be represented by each value. Table 4 also includes the depths to magnetic bottom — adjusted for sea depth for the marine point. The Curie isotherm depths calculated from heat flow data show a certain degree of correlation to the depths to magnetic bottom presented in Table 2 and Fig. 9. The depth in Africa of 15.4 km is quite close to the 16.9 km estimated from magnetic data; the Arabian depth estimate of 38.7 km is much deeper than the 17.6 km from magnetic data, whereas the Red Sea depth of 6.7 km is very close to the magnetic bottom estimates. Despite the complexities of the heat flow data themselves, these results provide an indication that the two depth estimation methods are broadly correlated and are probably mapping the same boundary.

Away from the active processes at the ocean ridge, the 1D and steady state assumptions are likely to be reasonably valid. Although the Red Sea is a narrow ocean, the oceanic crust is considerably wider than it is thick; hence geotherms will be generally of low angle and thermal structures close to 1D. Deviation from this case will occur close to active heat sources (e.g. concentrations of radiogenic material) or where thermal conductivity changes rapidly — e.g. in salt domes, but apart from the magmatic processes mentioned previously, these are likely to have little effect on heat flow and temperature at a whole crust scale. The oceanic crust is not in steady-state and cools with time ($\partial T/\partial t \neq 0$ in Eq. (10)), but the impact of this can be calculated by considering $\partial T/\partial t$ in an extended version of Eq. (13). If we assume that $\partial T/\partial t$ varies from 0 at the surface to 50 K/Ma at the Curie depth, calculations indicate that the modelled Curie depth would be ~5% deeper than using the steady state assumption. A value of 50 K/Ma appears to fit (e.g.) with the thermal models of Chappell and Kusznir (2008). Thus, we can say that in the context of the other assumptions made about thermal properties in this and the next method, the steady state assumption is generally reasonable.

6. Calculation of temperature–depth constrained geotherms

Mapping the depth to Curie isotherm using magnetic data only determines the temperature at one depth, but it is useful (for basin analysis, for example) to know the temperature at a range of depths.

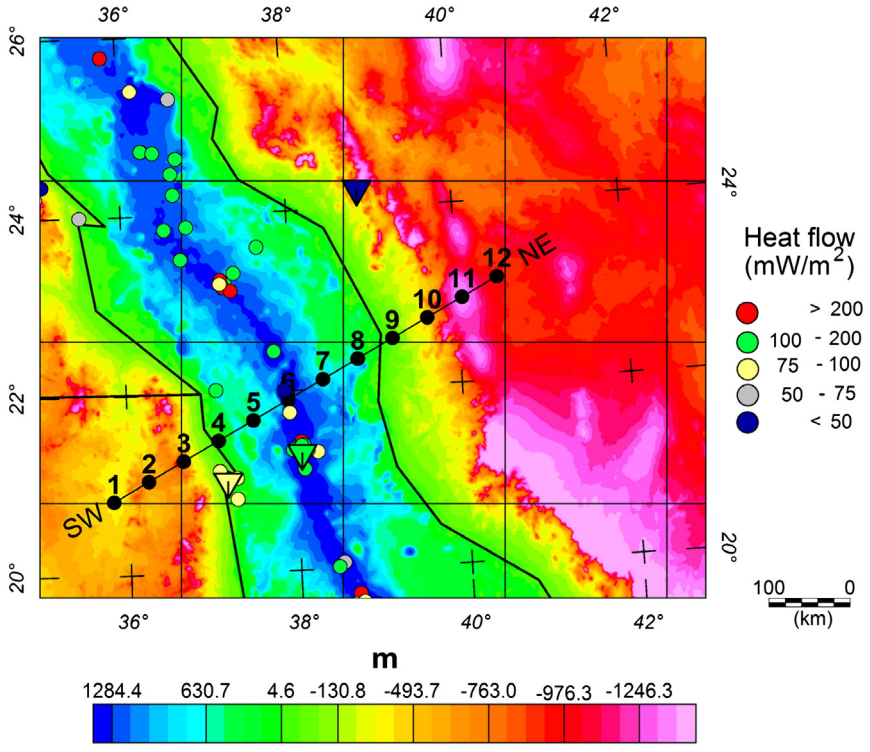

Fig. 10. Locations of heat flow stations (colour circles) are plotted on top of GEBCO bathymetry. Black dots represent the locations of the magnetic spectral analyses. Inverted triangles are the heat flow values (data points or averages) from which Curie depths have been estimated.

Please cite this article as: Salem, A., et al., Depth to Curie temperature across the central Red Sea from magnetic data using the de-fractal method, Tectonophysics (2014), http://dx.doi.org/10.1016/j.tecto.2014.04.027

Table 4
Depth to Curie isotherm results from heat flow data analysis — depths are below land surface or sea bed.

Location	Heat flow $mW \cdot m^{-2}$	Thermal conductivity of surface layer $W \cdot m^{-1} \cdot K^{-1}$	Heat production of surface layer $\mu W \cdot m^{-3}$	Thickness of surfaces layer km	Surface temperature °C	Depth to Curie isotherm below surface km	Mag depth below surface km
Africa #3–#4	96	2.22	1.54	0.81	27	15.4	16.9
Red Sea #6	160	1.25	1.25	2.00	22	6.7	6.4
Arabia #10	50	2.45	2.04	2.00	25	38.7	17.6

Particularly it is useful to know the depths at which critical temperatures for hydrocarbon maturity (generally in the range 60–180 °C) will occur in the crust. Predicting these temperatures (which are lower than the Curie temperature) requires interpolation of the geotherm (the relationship between temperature and depth) between the Curie isotherm depth and the surface; this in turn requires some estimates of thermal properties.

Linear interpolation between the Curie temperature and the surface would reflect a situation where there is constant thermal conductivity and no radiogenic heat production; once radiogenic heat production is added, the geotherm becomes curved; the curvature is proportional to the ratio of the radiogenic heat production A to the thermal conductivity k. In this study, we use a recently developed method of calculating 1D equilibrium or steady-state geotherms which uses deep temperature–depth constraints of any kind (e.g., the depth to Curie isotherm for a particular magnetic mineralogy or seismically determined temperature constraints from the depth of the thermal lithosphere, or other seismic or elastic lithosphere temperature–depth constraints) (Ravat et al., 2013). The formulation is based on a single layer of constant radiogenic heat production, A and constant thermal conductivity, k. Together with the surface heat flow Q_0 and the surface temperature T_0, these parameters can be used (e.g. Fowler, 2005) to define a quadratic curve of temperature T with depth z:

$$T = T_0 - \frac{A}{2k}z^2 + \frac{Q_0}{k}z. \tag{13}$$

In the forward modelling computations of the geotherm used in the previous section, the quantities A, k, Q_0 and T_0 are required to predict the temperature at depth. Since geotherms are customarily anchored or constrained only at the surface, the addition of the temperature–depth constraint at a deeper level applies an additional constraint to the geotherm and allows us to interpolate temperatures with greater confidence. Moreover, only two of the three parameters A, k and Q_0 need to be known or estimated and the other can be calculated. Thus, if Q_0 is known from measurements and k can be estimated based on the crustal terrain (Clauser and Huenges, 1995; Robertson, 1988), then A and the geotherm can be calculated. However, given Q_0, not all values of k will result in a valid (non-negative) value for A, so some iteration is required to yield credible values for both k and A (Clauser, 2011), but as a result we can also know the upper and lower bounds on both k and A. An additional guide to tuning these parameters in the continental regions is that the heat flow from the mantle should be in a reasonable range (~20–35 $mW \cdot m^{-2}$), depending on the tectonothermal age of the region.

We calculated these temperature–depth constrained geotherms in three places along our profile, to compare with the forward heat flow calculations in Table 4 — one in the centre of the Red Sea and two on the two margins of the continental areas on the either side of the rift in Sudan and Saudi Arabia. The thermal conductivity and heat flow values used to fit the geotherms to the magnetic derived Curie isotherm depths are given in Table 5 and the resulting geotherms and heat flow values are plotted in Fig. 11A and B. The radiogenic heat production rate derived for the central Red Sea (Table 5) is small and results in a nearly linear geotherm in the depth range of interest (sea bottom to the Curie isotherm). It is possible that all of the heat does not reach the surface by conduction in this tectonic scenario, but the importance of deriving the depth to the Curie isotherm from magnetic data is that it gives a temperature estimate at depth even in non-steady state situations. And the linear geotherm in these situations would yield the most conservative temperature estimates. The calculated geotherms from onshore Sudan and Saudi Arabia indicate the potential for geothermal energy — temperatures greater than 100 °C being reached at depths of around 2 km. Higher temperatures at shallow depths also provide scope for shallow hydrocarbon generation. According to Staplin (1977), the temperature ranges for hydrocarbon generation in the northern Red Sea are from 65 °C to 145 °C for oil and up to 165 °C for gas. These temperature ranges can be found at shallow depths in the central Red Sea area.

7. Discussion and conclusion

We have derived depths to magnetic bottom along a profile across the central Red Sea using the de-fractal spectral analysis method. This method applies a transformation to the observed magnetic field based on an estimated fractal index, such that the power spectrum resembles the power spectrum that would be generated by a random magnetisation distribution. From this transformed power spectrum, the depth to the top and bottom of the magnetic layer can be estimated — the latter being the Curie isotherm depth. The advantages of the present method with respect to the method of Bansal et al. (2011) are that the range of feasible de-fractal parameters can be estimated and the depth to the bottom of magnetic sources is obtained based on simultaneously estimating depth values from the centroid method and visual inspection of the forward modelling of the spectral peak. The centroid-method, used by itself, suffers from erroneous estimates in the presence of low wavenumber noise in the spectra.

The method has been applied to a profile of 12 100 km × 100 km windows of magnetic data in and around the central Red Sea and the 12 magnetic bottom depths show a clear pattern, consistent with the geologic evolution of the region, varying from 8.4 km in the rift area to about 19 km in the onshore areas. The method makes assumptions about the fractal nature of the magnetisation distribution within the crust; these assumptions are more realistic than assuming random magnetisation, but the fractal index becomes an additional parameter which needs to be estimated. It is clear, however, from inspection of

Table 5
Parameters used for the geotherm modelling using the Curie temperature–depth (from magnetic analysis) as a constraint. Depths are below land surface or sea bed.

Location/model parameters	Surface heat flow (q_s, $mW \cdot m^{-2}$)	Thermal conductivity (k, $W \cdot m^{-1} \cdot K^{-1}$)	Surface temp. (T_0, °C)	Depth to Curie isotherm (km)	Curie temp. (°C)	Heat production (A_0, $\mu W \cdot m^{-3}$)
Africa #3 and #4	96	2.10	27	16.9	580	3.2
Red Sea #6	160	1.80	22	6.4	580	0.96
Saudi Arabia #10	50	1.30	25	17.6	580	1.02

Please cite this article as: Salem, A., et al., Depth to Curie temperature across the central Red Sea from magnetic data using the de-fractal method, Tectonophysics (2014), http://dx.doi.org/10.1016/j.tecto.2014.04.027

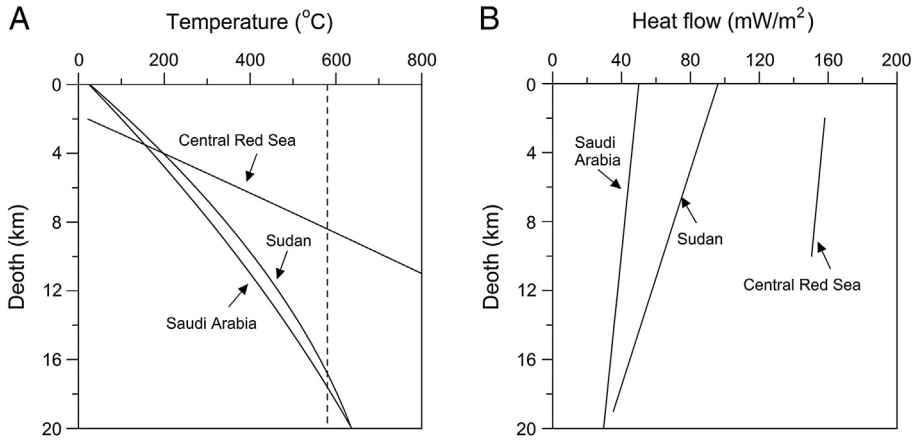

Fig. 11. (A) 1D, 1-layer geotherms for onshore Sudan, Central Rift, and onshore Saudi Arabia based on parameters in Table 5. (B) Heat flow variation with depth for the same model. Crustal values only are displayed.

the power spectra of the magnetic data (Figs. 5, 6 and 7) that the data themselves are in many cases diagnostic of the appropriate fractal index for the location. Even though this process is manual and will not give exactly repeatable results, the systematic variation of the interpreted fractal index, together with the generally consistent nature of the resulting magnetic bottom depths suggests that the de-fractal method is reasonably robust.

It should be noted that estimation of depth to magnetic sources using spectral analysis is affected by the data resolution. Our analysis was performed on a grid with different flight spacing and height. Given the fact that the flight height above bathymetry is much smaller than the flight line spacing, there are probably anomalies with wavelength smaller than 10 km that may be under-sampled by the survey and aliasing may occur. The change of resolution between offshore and onshore (flight line spacing of 2 km west of the Red Sea, 10 km above the Red Sea, and 500-800 m east of the Red Sea) can be seen in the map of magnetic anomalies in Fig. 4, although some of the change in dominant wavelength is due to changes in the depth of magnetic rocks. Such changes in spatial resolution may bias the results of the spectral method and may for instance explain why we obtained larger fractal index offshore in the Red Sea than onshore. The change of resolution could also explain why deeper top of magnetic sources is obtained using the tilt–depth method in the offshore area.

Comparison of depths to Curie isotherm derived from magnetic and heat flow approaches is restricted by the limited availability and reliability of heat flow data in the region. However, a few Curie isotherm depth estimates were made on the continents and in the Red Sea rift. The depths to Curie temperature derived from heat flow data show a close correlation with the magnetic bottom depths in Africa. In the central Red Sea rift the results are close, but the difficulty of identifying a representative heat flow value from the widely ranging heat flow observations, together with the problems of applying a heat flow conduction model in an area with strong convection systems means that no great weight can be assigned to this consistency. The heat flow observation in Arabia is also problematic due to its distance from the profile, so the discrepancy with the magnetic depth is not unexpected. Thus, it appears that our data and analysis suggest that the magnetic method is imaging the depths to Curie temperature in the Red Sea rift and on the African side of the rift the correlation between the two techniques is good and well supported.

Given the local variability of the heat flow observations and the distance of some of them from the magnetic profile, the observed difference in the results of the two depth to Curie temperature estimates is not unexpected. Each of the methods clearly has its own assumptions: the magnetic method relies on estimating the fractal index and assumes a constant fractal distribution of magnetisation; the heat flow method needs good estimates of thermal properties of the crust at all levels as well as reliable heat flow data. The combination of the two approaches in areas of better data should give good insights into the thermal structure of the Earth's crust. A new method of estimating crustal geotherms can use depths to Curie temperature as a constraint. This enables better calculation of temperatures through the crust above the Curie isotherm. The combination of these techniques should give better controlled thermal inputs to sedimentary basin modelling and geothermal exploration.

Along the 550 km profile of this study, the depths to Curie isotherm interpreted from magnetic data (considered most reliable in this case) vary from ~16–18 km along the flanks to ~8 km in the centre of the Red Sea; the shallowest Curie isotherm depths are observed over the oceanic crust and taper quite rapidly onto the continental areas, although there is still local variation within continents. This indicates that the highest mantle temperatures associated with this young oceanic rift are concentrated close to the area of oceanic crust. This fits in general terms with the results of Salem et al. (2013) who found that the smallest Moho density contrast was concentrated in this area and the sub-Moho velocities of Egloff et al. (1991) which were most significantly reduced in the centre of the Red Sea — tapering to near-normal velocities at the coastline. The fact that the high crustal temperatures appear to be even more concentrated around the oceanic zone suggests that this may be a transient effect and that the Curie isotherm may shallow in time below the continental margins; an effect that would be expected to be counteracted by the general cooling of the system away from the oceanic ridge. Inspection of the interpolated geotherms (Fig. 11A) indicates that the range of depths for hydrocarbon maturity (Staplin, 1977) is ~1–3 km at the African end of the profile and ~1–4 km at the Arabian end. More reliable heat flow data would be expected to improve confidence in these ranges, but thick accumulations of sediment would also impact the depth of the hydrocarbon window.

Acknowledgements

We are indebted to Dr. Richard Blakely for his discussions and comments on the idea of the paper. We also thank an anonymous reviewer and Dr. Bouligand for comments and suggestions, which helped greatly in improving the manuscript. The techniques used in this study were developed as part of a joint depth to Curie temperature study implemented primarily by Getech and funded by Shell. The method of computing geotherms using temperature-depth constraints was developed by DR with a grant from the US National Science Foundation (EAR-1246921).

References

ArRajehi, A., McClusky, S., Reilinger, R., Daoud, M., Alchalbi, A., Ergintav, S., Gomez, F., Sholan, J., Bou-Rabee, F., Ogubazghi, G., Haileab, B., Fisseha, S., Asfaw, L., Mahmoud, S., Rayan, A., Bendik, R., Kogan, L., 2010. Geodetic constraints on present day motion of the Arabian Plate: implications for Red Sea and Gulf of Aden rifting. Tectonics 29, TC3011.

Bansal, A.R., Gabriel, G., Dimri, V.P., Krawczyk, C.M., 2011. Estimation of depth to the bottom of magnetic sources by a modified centroid method for fractal distribution of sources: an application to aeromagnetic data in Germany. Geophysics 76, L11–L22.

Bassin, C., Laske, G., Masters, G., 2000. The current limits of resolution for surface wave tomography in North America. EOS Trans. Am. Geophys. Union 81 (48) (Fall Meet Suppl., Abstract S12A-03).

Bastow, I.D., Keir, D., 2011. The protracted development of the continent–ocean transition in Afar. Nat. Geosci. 4, 248–250.

Bhattacharyya, B.K., Leu, L., 1975. Analysis of magnetic anomalies over Yellowstone National Park. Mapping the Curie-point isotherm surface for geothermal reconnaissance. J. Geophys. Res. 80, 461–465.

Bhattacharyya, B.K., Leu, L., 1977. Spectral analysis of gravity and magnetic anomalies due to rectangular prismatic bodies. Geophysics 42, 41–50.

Blakely, R.J., 1988. Curie temperature isotherm analysis and tectonic implications of aeromagnetic data from Nevada. J. Geophys. Res. 93 (11), 832 (817-11).

Blakely, R.J., 1995. Potential Theory in Gravity and Magnetic Applications. Cambridge University Press, Cambridge, U. K.

Bosworth, W., Huchon, P., McClay, K., 2005. The Red Sea and Gulf of Aden basins. J. Afr. Earth Sci. 43, 334–378.

Bouligand, C., Glen, J.M.G., Blakely, R.J., 2009. Mapping Curie temperature depth in the western United States with a fractal model for crustal magnetization. J. Geophys. Res. 114, B11104 (Issue).

CCGM (Commission for the Geological Map of the World), 2000. Geological map of the world, 2nd edition.

Chappell, A.R., Kusznir, N.J., 2008. Three-dimensional gravity inversion for Moho depth at rifted continental margins incorporating a lithosphere thermal gravity anomaly correction. Geophys. J. Int. 174, 1–13.

Clauser, C., 2011. Radiogenic heat production of rocks. In: Gupta, H. (Ed.), Encyclopedia of Solid Earth Geophysics. Springer, pp. 1018–1024.

Clauser, C., Huenges, E., 1995. Thermal conductivity of rocks and minerals. A Handbook of Physical Constants, Rock Physics and Phase Relations, AGU Reference Shelf. Am. Geophys. Union, 3, pp. 105–126.

Connard, G., Couch, R., Gemperle, M., 1983. Analysis of aeromagnetic measurements from the Cascade Range in central Oregon. Geophysics 48, 376–390.

Davis, E.E., Lister, C.R.B., 1974. Fundamentals of ridge crest topography. Earth Planet. Sci. Lett. 21, 405–413.

Egloff, F., Rihm, R., Makris, J., Izzeldin, Y.A., Bobsein, M., Meier, K., Junge, P., Noman, T., Warsi, W., 1991. Contrasting structural styles of the eastern and western margins of the southern Red Sea: the 1988 SONNE experiment. Tectonophysics 198, 329–353.

Fedi, M., Quarta, T., De Santis, A., 1997. Inherent power law behavior of magnetic field power spectra from a Spector and Grant ensemble. Geophysics 62, 1143–1150.

Fowler, C.M.R., 2005. The Solid Earth: An Introduction to Global Geophysics. Cambridge Univ. Press (685 pp.).

Getech, 1992. The African magnetic mapping project — commercial report (unpublished).

Girdler, R.W., Evans, T.R., 1977. Red Sea heat flow. Geophys. J. Int. 51 (Issue 1), 245–251.

Green, C.M., Barritt, S.D., Fairhead, J.D., Misener, D.J., 1992. The African magnetic mapping project. Extended Abstract, EAEG 54th Meeting and Technical Exhibition, Paris.

Hemant, K., Mitchell, A., 2009. Magnetic field modelling and interpretation of the Himalayan–Tibetan plateau and adjoining north Indian plains. Tectonophysics 478, 87–99.

Kolmogorov, A.N., 1941. Local structure of turbulence in an incompressible fluid at very high Reynolds numbers. Dokl. Akad. Nauk SSSR 30, 299–303.

Mandelbrot, B.B., 1983. The Fractal Geometry of Nature. W.H. Freeman, New York, NY.

Manea, M., Manea, V.C., 2011. Curie point depth estimates and correlation with subduction in Mexico. Pure Appl. Geophys. 168, 1489–1499.

Maus, S., Dimri, V.P., 1994. Scaling properties of potential fields due to scaling sources. Geophys. Res. Lett. 21, 891–894.

Maus, S., Dimri, V.P., 1995. Potential field power spectrum inversion for scaling geology. J. Geophys. Res. 100 (12), 605–612 (616).

Maus, S., Gordon, D., Fairhead, D.J., 1997. Curie temperature depth estimation using a self-similar magnetization model. Geophys. J. Int. 129, 163–168.

Mogren, S.M.A., 2004. Geophysical Investigations of the Najd Fault System. (PhD thesis) University of Leeds UK p. 209.

Nataf, H.C., Richard, Y., 1996. 3SMAC: an a priori tomographic model of the upper mantle based on geophysical modelling. Phys. Earth Planet. Inter. 95, 101–122.

Okubo, Y., Graf, R.J., Hansen, R.O., Ogawa, K., Tsu, H., 1985. Curie point depths of the island of Kyushu and surrounding areas, Japan. Geophysics 50, 481–494.

Pilkington, M., Todoeschuck, J.P., 1993. Fractal magnetization of continental crust. Geophys. Res. Lett. 20, 627–630.

Pilkington, M., Todoeschuck, J.P., 1995. Scaling nature of crustal susceptibilities. Geophys. Res. Lett. 22, 779–782.

Pilkington, M., Gregotski, M.E., Todoeschuck, J.P., 1994. Using fractal crustal magnetization models in magnetic interpretation. Geophys. Prospect. 42, 677–692.

Pollack, H.N., 1992. Global Heat Flow Data Set. World Data Centre A for Solid Earth Geophysics. NOAA.

Rajaram, M., Anand, S.P., Hemant, K., Purucker, M.E., 2009. Curie isotherm map of Indian subcontinent from satellite and aeromagnetic data. Earth Planet. Sci. Lett. 281 (Issue 3–4), 147–158.

Ravat, D., Pignatelli, A., Nicolosi, I., Chiappini, M., 2007. A study of spectral methods of estimating the depth to the bottom of magnetic sources from near-surface magnetic anomaly data. Geophys. J. Int. 169, 421–434.

Ravat, D., Salem, A., Abdelnaby, A., Elawdi, E., Morgen, P., 2011. Probing magnetic bottom and crustal temperature variations along the Red Sea margin of Egypt. Tectonophysics 510, 337–344.

Ravat, D., Salem, A., Lowry, A., Schutt, D., 2013. Geotherms from the Curie depth constrained solutions of the one dimensional steady-state heat flow equation. Earth Scope National Meeting, Raleigh, North Carolina, May 12–15.

Robertson, E.C., 1988. Thermal properties of rocks. U.S. Geological Survey Open-file Report 88–441. U.S. Geological Survey, Reston (106 pp.).

Ross, H.E., Blakely, R.J., Zoback, M.D., 2006. Testing the use of aeromagnetic data for the determination of Curie depth in California. Geophysics 71, L51–L59.

Roy, R.F., Beck, A.E., Touloukian, Y.S., 1981. Thermophysical properties of rocks. In: Touloukian, Y.S., Judd, W.R., Roy, R.F. (Eds.), Physical Properties of Rocks and Minerals. McGraw-Hill, New York, N.Y., pp. 409–502.

Salem, A., Ushijima, K., Elsirafi, A., Mizunaga, H., 2000. Spectral analysis of aeromagnetic data for geothermal reconnaissance of Quseir area, northern Red Sea, Egypt. Proceedings of World Geothermal Congress. Kyushu-Tohoku, Japan, pp. 1669–1673.

Salem, A., Williams, S., Fairhead, J.D., Ravat, D., Smith, R., 2007. Tilt–depth method: a simple depth estimation method using first-order magnetic derivatives. Lead. Edge 26, 1502–1505.

Salem, A., Green, C., Campbell, S., Fairhead, J.D., Cascone, L., Moorhead, L., 2013. Moho depth and sediment thickness estimation beneath the Red Sea derived from satellite and terrestrial gravity data. Geophysics 78, G89–G101.

Shuey, R.T., Schellinger, D.K., Tripp, A.C., Alley, L.B., 1977. Curie depth determination from aeromagnetic spectra. Geophys. J. Int. 50, 75–101.

Spector, A., Grant, S., 1970. Statistical models for interpreting aeromagnetic data. Geophysics 35, 293–302.

Staplin, F.L., 1977. Interpretation of thermal history from color of particulate organic matter—a review. Paleontology 1, 9–18.

Stein, C.A., Stein, S., 1992. A model for the global variation in oceanic depth and heat flow with lithospheric age. Nature 359, 123–129.

Tanaka, A., Okubo, Y., Matsubayashi, O., 1999. Curie point depth based on spectrum analysis of the magnetic anomaly data in East and Southeast Asia. Tectonophysics 306, 461–470.

Wasilewski, P.J., Thomas, H.H., Mayhew, M.A., 1979. Moho as a magnetic boundary. Geophys. Res. Lett. 6 (7), 541–544.

White, R.S., McKenzie, D., O'Nions, R.K., 1992. Oceanic crustal thickness from seismic measurements and rare earth element inversions. J. Geophys. Res. 97 (B13), 19683–19715.

Please cite this article as: Salem, A., et al., Depth to Curie temperature across the central Red Sea from magnetic data using the de-fractal method, Tectonophysics (2014), http://dx.doi.org/10.1016/j.tecto.2014.04.027